Inhomogeneous MUSIG Model – a Population Balance Approach for Polydispersed Bubbly Flows

Eckhard Krepper[1], Thomas Frank[2], Dirk Lucas[1], Horst-Michael Prasser[3], Philip J. Zwart[4]

[1]Forschungszentrum Dresden-Rossendorf (FZD), Institute of Safety Research,
PO Box 510119, D-01314 Dresden, Germany, E.Krepper@fzd.de; D.Lucas@fzd.de

[2]ANSYS Germany, [3]ETH-Zürich, [4]ANSYS Canada

Keywords: Bubbly flow, CFD, Non drag forces, bubble break up, bubble coalescence, population balance, validation

Abstract

A generalized inhomogeneous Multiple Size Group (MUSIG) Model based on the Eulerian modeling framework was developed in close cooperation of ANSYS-CFX and Forschungszentrum Dresden-Rossendorf and implemented into CFX-10. Simulating a poly-dispersed gaseous liquid two phase flow along with the mass exchanged between bubble size classes by bubble coalescence and bubble break-up and the momentum exchange of bubble size dependent bubble forces have to be considered. Particularly the lift force has been proved to play an important role establishing a certain flow regime. The paper describes the main concepts of the model approach and presents a model validation case. Further application test cases are presented by Krepper et al. 2007.
The inhomogeneous MUSIG model approach was shown to be able to describe of bubbly flow with higher gas content. Particularly the separation phenomenon of small and large bubbles which was proven to be a key phenomenon for the establishment of the corresponding flow regime is well described. Weaknesses in this approach can be attributed to the characterization of bubble coalescence and bubble break-up, which must be further investigated.

1. Introduction

Many flow regimes in Nuclear Reactor Safety Research are characterized by multiphase flows, with one phase being a continuous liquid and the other phase consisting of gas or vapour of the liquid phase. The flow regimes found in vertical pipes are dependent on the void fraction of the gaseous phase, which vary from bubbly flows at low fractions to higher void fraction regimes of slug flow, churn turbulent flow, annular flow and finally to droplet flow. In the regime of bubbly and slug flow the multiphase flow shows a spectrum of different bubble sizes. While disperse bubbly flows with low gas volume fraction are mostly mono-disperse, an increase of the gas volume fraction leads to a broader bubble size distribution due to break-up and coalescence of bubbles. Bubbles of different sizes are subject to lateral migration due to forces acting in lateral direction, which is different from the main drag force direction. The bubble lift force was found to change the sign as the bubble size varies. Consequently this lateral migration leads to a radial de-mixing of small and large bubbles and to further coalescence of large bubbles migrating towards the pipe center into even larger Taylor bubbles or slugs.
An adequate modeling approach must to consider all these phenomena. The paper presents a generalized inhomogeneous Multiple Size Group (MUSIG) Model based on the Eulerian modeling framework. Within this model the dispersed gaseous phase is divided into N inhomogeneous velocity groups (phases) and each of these groups is subdivided into M_j bubble size classes. Bubble break-up and coalescence processes between all bubble size classes M_j are taken into account by appropriate models.

2. Nomenclature

C_D	drag coefficient
C_L	lift coefficient
d_b	volume equivalent bubble diameter (m)
d_h	horizontal bubble diameter (m)
D	pipe diameter (m)
Eo	Eötvös Number
F_B	break-up coefficient
F_C	coalescence coefficient
F_L	lift force (N m^{-3})
g	acceleration due to gravity (m s^{-2})
J	superficial velocity (m s^{-1})
P	pressure (Pa)
Re	bubble Reynolds Number
w	velocity (m s^{-1})

Greek letters

α	gas volume fraction
ρ	density (kg m^{-3})
σ	surface tension (N m^{-1})

Subscripts

g	gas
l	liquid

3. The Lift Force and Influence on the Flow Regime

Simulating a two-phase flow applying the Euler/Eulerian approach, the momentum exchange between the phases has to be considered. Apart from the drag acting in flow direction, the so called non-drag forces acting perpendicularly to the flow direction must to be considered. Namely the lift force, the turbulence dispersion force and the wall force play an important role. Here the influence of the lift force will be discussed.

3.1. Lift force inversion in a poly-disperse bubbly flow

The lift force considers the interaction of the bubble with the shear field of the liquid. Related on the unit volume it can be calculated as:

$$\vec{F}_L = -C_L \rho_l \alpha (\vec{w}_g - \vec{w}_l) \times rot(\vec{w}_l) \qquad (1)$$

The classical lift force, which has a positive coefficient C_L, acts in the direction of decreasing liquid velocity. In case of co-current upwards pipe flow this is the direction towards the pipe wall. Numerical (Ervin and Tryggvason, 1997, Bothe et al., 2006) and experimental (Tomiyama et al., 1995) investigations showed, that the direction of the lift force changes its sign, if a substantial deformation of the bubble occur. Tomiyama (1998) investigated single bubble motion and derived the following correlation for the coefficient of the lift force from these experiments:

$$C_L = \begin{cases} \min[0.288\tanh(0.121\,\mathrm{Re}),\ f(Eo_d)] & Eo_d < 4 \\ f(Eo_d) \quad for & 4 < Eo_d < 10 \\ -0.27 & Eo_d > 10 \end{cases} \qquad (2)$$

$$with \quad f(Eo_d) = 0.00105 Eo_d^3 - 0.0159 Eo_d^2 - 0.0204 Eo_d + 0.474$$

This coefficient depends on the modified Eötvös number given by:

$$Eo_d = \frac{g(\rho_l - \rho_g) d_h^2}{\sigma} \qquad (3)$$

Here d_h is the maximum horizontal dimension of the bubble. It is calculated using an empirical correlation for the aspect ratio by Wellek et al. (1966) with the following equation:

$$d_h = d_b \sqrt[3]{1 + 0.163 Eo^{0.757}} \qquad (4)$$

Figure 1 represents the dependency of C_L on the bubble size in eq. (2) for an air/water system at ambient conditions. For this case C_L changes its sign at a bubble diameter of d_b=5.8 mm.

The MTLoop experiments performed at FZD (Prasser et al. 2002) have shown the lift force to also reverse also in a poly-disperse bubbly flow. Radial void fraction distributions show a wall peak for bubbles below the critical diameter, while bubbles with a bigger diameter form a central void fraction peak. This is independent from the general type of the profile of the total void fraction, i.e. a wall-peak for the small bubble fraction is found also in case of a pronounced central peaked void fraction profile.

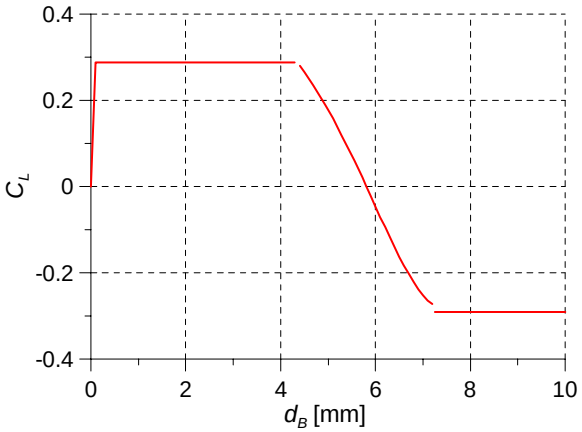

Figure 1: Lift coefficient for air/water according to eq. (2)

The FZD facility TOPFLOW has significantly extended the experimental opportunities to study this effect. It was shown that the described effects are present also in a large diameter pipe. The vanishing of the wall peak in gas fraction profiles that are subdivided into narrow bubble-size classes of 0.5 mm class-width is observed at a diameter close to the value given by Tomiyama. For an air-water flow at ambient conditions, the equivalent critical bubble diameter is 5.5 mm. As shown in Fig. 3, bubble of this size still display a pronounced wall peak vanising at about 6 - 6.5 mm bubble diameter. The fact that a wall peak is still present for bubbles slightly larger than the Tomiyama diameter results from their continuous production by coalescence events, which are frequent in the peak region between bubbles below the critical size.

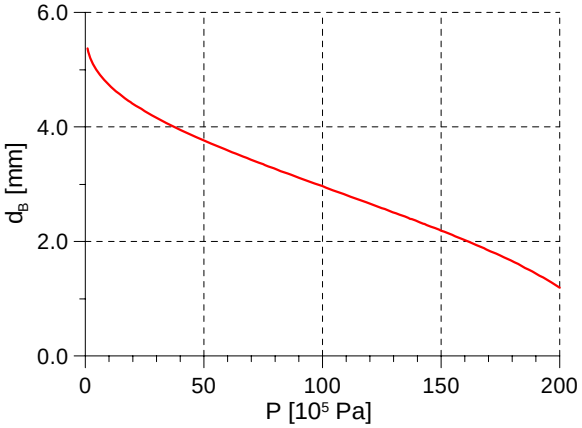

Figure 2: Decrease of the critical equivalent bubble diameter of the lift force inverse for steam/water with growing saturation pressure

An important merit of the TOPFLOW experiments is the possibility to check the correctness of the Tomiyama model at high pressures and temperatures. The critical diameter is scaled by increases with the modified Eötvös number according eq. (3). Keeping in view that the surface tension decreases with growing saturation temperature, the critical bubble diameter is expected to be lower for the steam-water tests. The dependency is given in Fig. 2. This was confirmed by the measurements, as shown in Fig. 3 (right side), where decomposed gas fraction profiles in the close-to-wall region are plotted for a saturation pressure of 6.5 MPa. A wall peak is only found for bubbles below 3.5 mm, which is in agreement with the dependency of the critical diameter from pressure in Fig. 2.

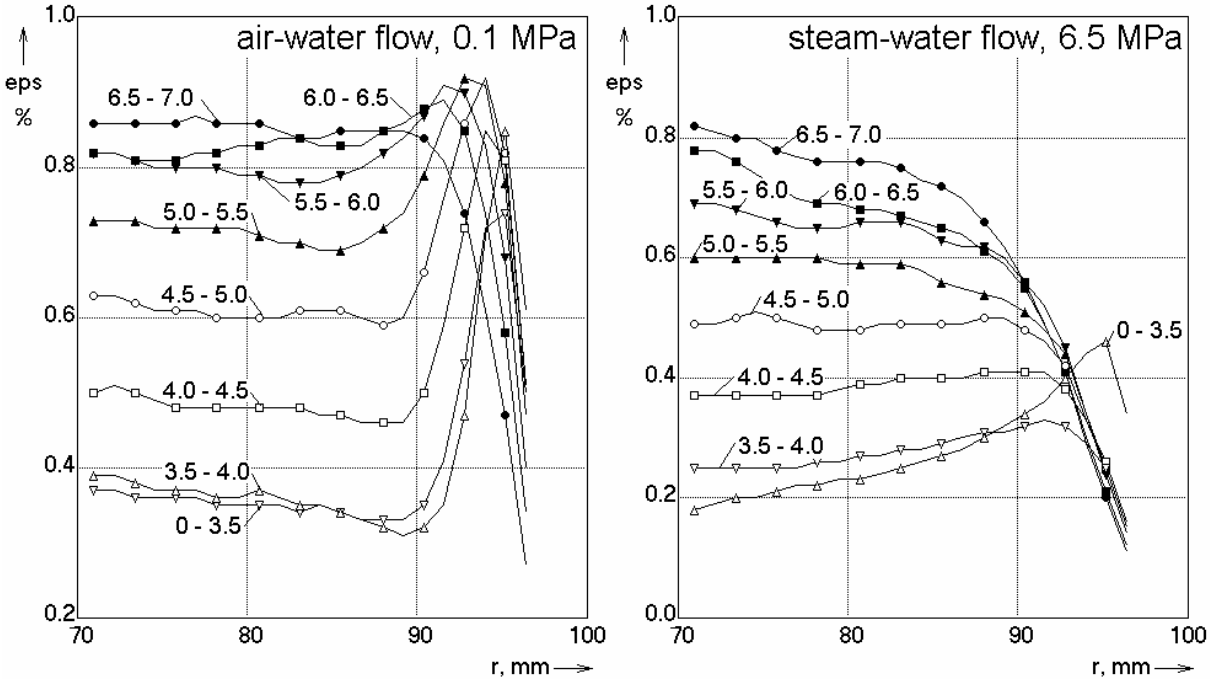

Figure 3: Gas fraction profiles decomposed according to bubble size classes in the test pipe DN200 at J_L = 1.017 m/s and J_G = 0.219 m/s, L/D = 39.7, gas injection orifices: D_{inj} = 4 mm (Prasser et al. 2007)

3.2. Development of the flow along a vertical pipe – radial separation of large and small bubbles

The evolution of the flow along the pipe is determined by a complex interaction between bubble forces, which cause a lateral bubble migration and bubble coalescence and break-up. Also the transition from bubbly to slug flow is influenced by this interaction. As mention above the lift force causes, that small bubbles (diameter < ca. 5.8 mm in case of air-water flow) can be found preferably in the wall region, while larger bubbles are accumulated in the core region. This separation of small and large bubbles clearly influences the development of the flow, since bubble coalescence and break-up depend on the local bubble densities (see Prince and Blanche 1990, Luo and Svendsen 1996). On the other hand the dissipation rate of turbulent energy is clearly larger in the near wall region than in the core flow. The consequences for the transition to slug flow can be explained by help of Fig. 4. An upward air-water flow is considered. In both considered cases small bubbles (diameter < 5.5 mm) are injected. In the left side of the figure a low superficial gas velocity was assumed. The small bubbles tend to move towards the wall. The local gas fraction in the wall region is larger than the averaged gas fraction, but it is still low. In this case bubble coalescence and break-up are in equilibrium and a stable bubble flow is established.

If the gas superficial velocity is increased (Fig. 4, right side), the equilibrium between bubble coalescence and break-up is shifted towards a larger bubble diameter, because the coalescence rate increases with the square of the bubble density, while the break-up rate is only proportional to the bubble density. The bubble break-up rate strongly increases with the bubble diameter.

By a further increase of the gas superficial velocity, more and more large bubbles (diameter > 5.5 mm) are generated. They start to migrate towards the pipe centre. If enough large bubbles are generated by coalescence in the wall region, some of them can reach the core region without break-up. Because of the lower dissipation rate of turbulent energy they can then growth up by further coalescence at much lower break-up rates, typical for the low shear in the centre.

This mechanism is the key for the transition from bubble to slug flow. That means, for an appropriate modelling of the transition a number of bubble classes as well as radial gas fraction profiles for each bubble class have to be considered.

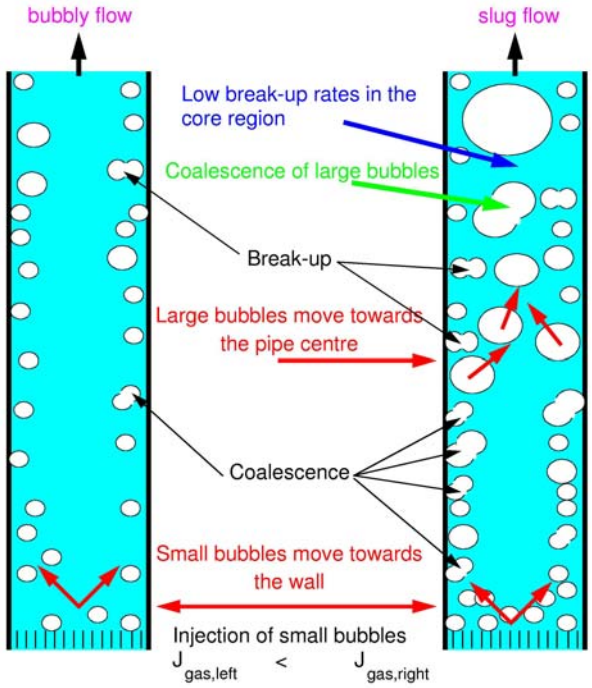

Figure 4: Stable bubble flow (left) and transition to slug flow (right)

4. Multiple Size Group Approach

4.1. The MUSIG model by Lo

For larger gas volume fractions, several bubble size classes that include the exchange of mass caused by bubble coalescence and break-up phenomena have to be considered. In principle, the two fluid approach described above can be extended to simulate a continuous liquid phase and several gaseous dispersed phases solving the complete set of balance equations for each phase. The investigations however showed that for an adequate description of the gas volume fraction profile including a population balance model decades of bubble size classes would be necessary. In a CFD code, such a procedure is limited by the increased computational effort to obtain converged flow solutions.

To solve this problem, the multiple size group model implemented by the code developer in CFX-4 solves only one common momentum equation for all bubble size classes (homogeneous MUSIG model, see Lo 1996). Mathematically, the Multiple Size Group model MUSIG is based on the population balance method and the two-fluid modelling approach. The dispersed phase is divided into M size fractions. The population balance equation is applied to describe the mass conservation of the size fractions taking into account of the inter-fraction mass transfer resulting from bubble coalescence and break-up. This model approach allows a sufficient number of fraction size groups required for the coalescence and break-up calculation to be used and has found a number of successful applications to large-scale industrial multiphase flow problems.

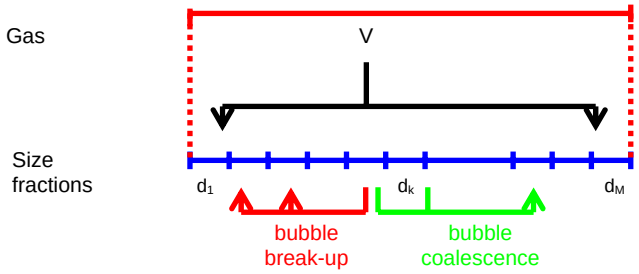

Figure 5: Schema of the standard MUSIG model: All size fractions representing different bubble sizes moves in the same velocity field

Nevertheless, the assumption also restricts its applicability to homogeneous dispersed flows where the slip velocity of particles are approximately independent of particle size and the particle relaxation time is sufficiently small relative to inertial time scales. Thus, the asymptotic slip velocity can be considered to be attained almost instantaneously. The homogeneous MUSIG model described above fails to predict the correct phase distribution when heterogeneous particle motion becomes important. One example is the bubbly flow in vertical pipes where the non-drag forces play an essential role on the bubble motion. In the previous chapter the lift force was described to change its sign, when applied for large deformed bubbles, which are dominated by the asymmetrical wake. The lift force in this case has a direction opposite to the shear induced lift force on a small bubble. For this reason, large bubbles tend to move to the pipe core region resulting in a core void maximum whereas a wall void peak is measured for small bubbles. The radial separation of small and large bubbles cannot be predicted by the homogeneous MUSIG model. This has been shown to be a key mechanism for the establishment of a certain flow regime as discussed earlier in chapter 2.

4.2. New strategies – the inhomgeneous MUSIG model

A combination of the consideration of different dispersed phases and the algebraic multiple size group model was proposed to combine both the adequate number of bubble size classes for the simulation of coalescence and break-up and a limited number of dispersed gaseous phases to limit the computational effort (Krepper et al. 2005). The inhomogeneous MUSIG model was developed in cooperation with ANSYS CFX and is implemented in CFX-10 (Shi et al. 2004, Zwart et al. 2003, Frank et al. 2005).

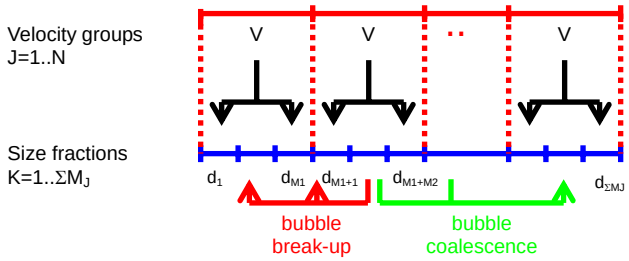

Figure 6: Improvement of the polydispersed approach: The size fractions M_j are assigned to the velocity field Vj

In the inhomogeneous MUSIG model the gaseous disperse phase is divided into a number N so-called velocity groups (or phases), where each of the velocity groups is characterized by its own velocity field. Further, the overall bubble size distribution is represented by dividing the bubble diameter range within each of the velocity groups *j* in a number M_j j=1..*N* bubble sub-size fractions. The population balance model considering bubble coalescence or bubble break-up is applied to the sub-size groups (see Fig. 6). Hence the mass exchange between the sub-size groups can exceed the boundaries of the velocity groups.
The lower and upper boundaries of bubble diameter intervals for the bubble size fractions can be controlled by either an equal bubble diameter distribution, an equal bubble mass distribution or can be based on user definition of the bubble diameter ranges for each distinct bubble diameter fraction. The subdivision should be based on the physics of bubble motion for bubbles of different size, e.g. different behavior of differently sized bubbles with respect to lift force or turbulent dispersion. Therefore, it can be suggested that in most cases *N*=2 or 3 velocity groups are sufficient in order to capture the main phenomena in bubbly or slug flows.
The continuum equation for the gaseous dispersed phase *j* can be written as:

$$\frac{\partial}{\partial t}\left(\alpha_j \rho_g\right) + \nabla \cdot \left(\alpha_j \rho_g \vec{U}_j\right) = S_j \qquad (5)$$

the momentum equation for the j^{th} gaseous phase has the form:

$$\frac{\partial}{\partial t}\left(\alpha_j \rho_g \vec{U}_j\right) + \nabla \cdot \left(\alpha_j \rho_g \vec{U}_j \times \vec{U}_j\right) = \nabla \cdot \left(\alpha_j \mu_g \left(\nabla \vec{U}_j + \left(\nabla \vec{U}_j\right)^T\right)\right) \quad (6)$$
$$-\alpha_j \nabla p + \alpha_j \rho_g \vec{g} + \vec{M}_j + \vec{S}_{Mj}$$

with

$$\vec{F}_j = \vec{F}_{j,D} + \vec{F}_{j,L} + \vec{F}_{j,W} + \vec{F}_{j,TD} \quad (7)$$

where αj, ρg, μg are the void fraction, density and viscosity of the gas and $\vec{F}_j$ represents the sum of interfacial forces like the drag force $F_{j,D}$, lift force $F_{j,L}$, wall lubrication force $F_{j,W}$ and turbulent dispersion force $F_{j,TD}$. The term, $\vec{S}_{Mj}$, represents the transfer of gaseous phase momentum between different velocity groups due to bubble break-up and coalescence processes that causes bubbles of certain size to switch to a different velocity group.
Additional for each sub-size fraction, *i*, (i=1..M_j) in the velocity group *j* $f_i\alpha_j$ the continuum equation has to be solved:

$$\frac{\partial}{\partial t}\left(f_i \alpha_j \rho_g\right) + \nabla \cdot \left(f_i \alpha_j \rho_g \vec{U}_j\right) = S_{ij} \quad (8)$$

The source terms, S_{ij}, represent the local transfer of gaseous phase mass due to bubble break-up and coalescence processes. They can be assigned to S_k, which are the elements of the population balance model. Note that the above equations the index *j* extends over the range 1..*N* and the index *k* over the range 1.. $\sum_{j=1}^{N} M_j$. The population balance equations have then the form:

$$S_k = B_{k,B} - D_{kB} + B_{kC} - D_{kC} \quad (9)$$

where $B_{k,B}$ is the bubble birth rate due to break-up of larger bubbles, $D_{k,B}$ is the bubble death rate due to break-up of bubbles from size group k into smaller bubbles, $B_{k,C}$ is the bubble birth rate into size group *k* due to coalescence of smaller bubbles to bubbles belonging to size group *k* and finally $D_{k,C}$ is the bubble death rate due to coalescence of bubbles from size group *k* with other bubbles to even larger ones. The inhomogeneous MUSIG model approach does not presume a certain coalescence or break-up model. As an example the validation calculations presented in the chapter 4 and 5 were performed applying the break-up model of Luo and Svendsen (1996) and the bubble coalescence model of Prince and Blanch (1990).

5. Model validation by means of two phase upward flow in vertical pipes - Tests with higher gas volume fraction

Gas-liquid flow in vertical pipes is a very good object for studying the phenomena of two-phase flows. In case of bubbly flows the bubbles move under clear boundary conditions, resulting in a shear field of constant and well-known structure where the bubbles rise for a comparatively long time. This allows studying the lateral motion of the bubbles in a shear flow by comparing gas distributions measured at different heights.

5.1. Simulation of different dispersed phases

For the test 118 in the MT-loop experiments (J_L=1.017 m/s, J_G=0.219 m/s) air was injected by nozzles equally distributed over the tube cross section. At the upper end of the tube, a radial gas volume fraction according to Fig. 7a and a bubble size distribution according to Fig. 7b were found.

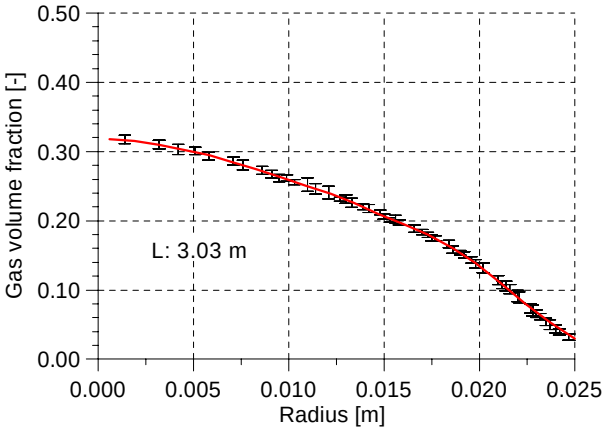

a) radial gas fraction distribution

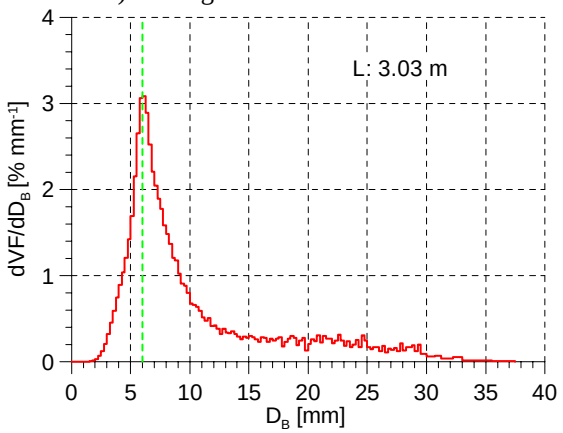

b) bubble size distribution

Figure 7: Measured radial gas fraction distribution and bubble size distribution for the test 118 (J_L=1.017 m/s, J_G=0.219 m/s)

To describe a bubbly flow showing a core gas fraction peak according Fig. 7a several dispersed phases with each having its own velocity field were simulated. As a first step the mass exchange between the gas phases was excluded. Simulations with 2, 3 and 4 different bubble size classes were performed to investigate the necessary number of dispersed phases for an adequate simulation. According to the measured bubble size distribution at the upper end of the tube (Fig. 7b) the fraction and the averaged bubble size of each bubble size class was determined and given as an inlet condition (see Table 1). The selection of the range boundaries was performed considering the dependency of the lift coefficient on the bubble size. In the simulation only the dependence of the bubble forces on the bubble size – particularly the lift force was considered. The resulting radial gas fraction distributions for the variants are shown in Fig. 8.

Table 1: Parameters of the simulations with several dispersed gas phases					
2 classes	range	0 - 6		>6	
	av. diameter	4.95		12.55	
	gas fraction	0.4185		0.12358	
3 classes	range	0 – 4.5	4.5 – 7.5		>7.5
	av. diameter	3.76	6.09		15.02
	gas fraction	0.01136	0.06707		0.08698
4 classes	range	0 – 4.5	4.5 - 6	6 – 7.5	>7.5
	av. diameter	3.76	5.39	6.68	15.02
	gas fraction	0.01136	0.03050	0.03661	0.08698

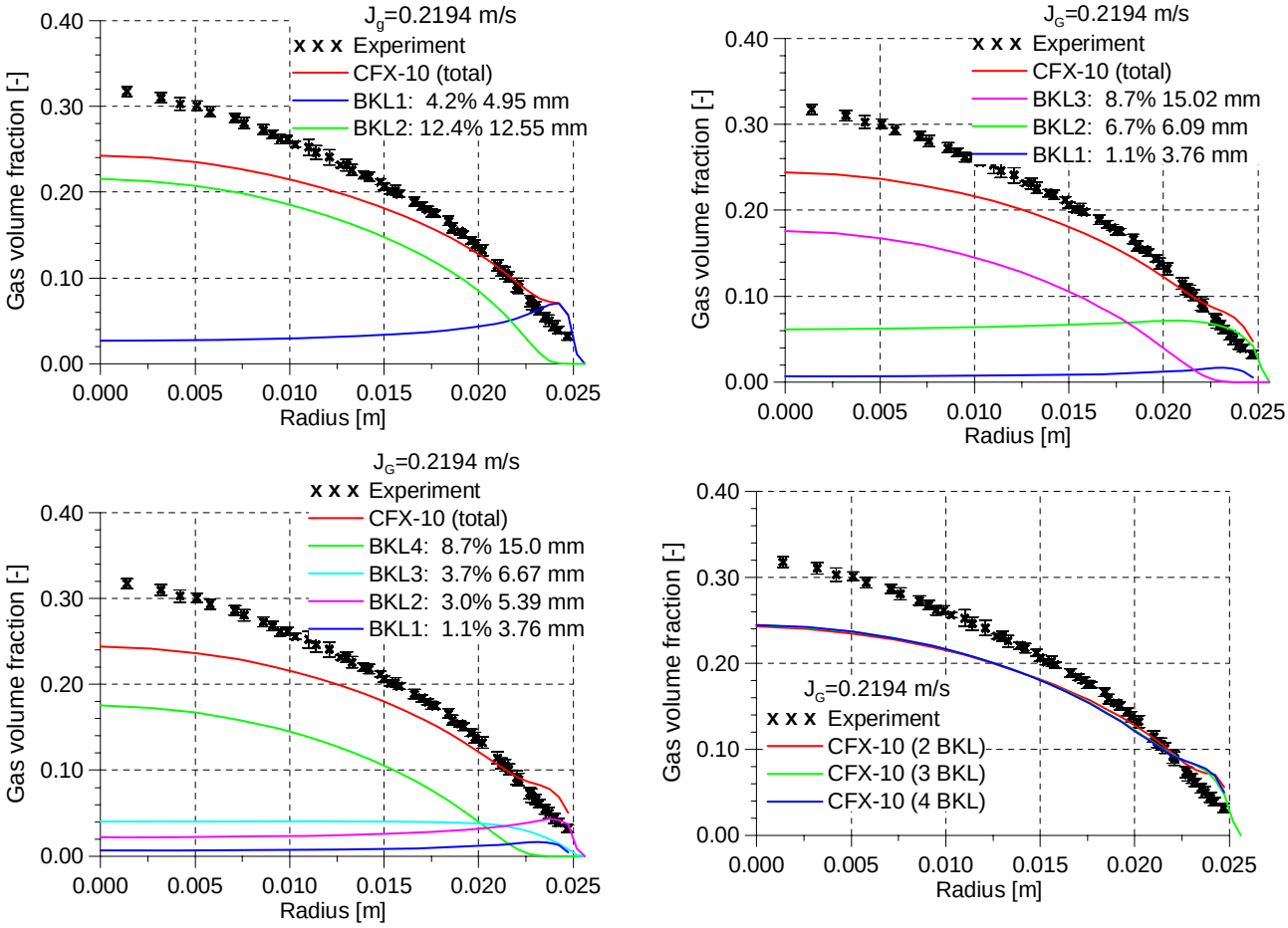

Figure 8: Radial gas fraction profiles for simulation with different dispersed phases

The expected dependencies were observed, i.e. for the classes with small bubbles a wall peak and for bubble size classes with large bubbles a core peak is found. The total values correspond to the measured values. However, according to Fig. 6.2d almost no difference between the investigated three cases was found. The improved physical representation of the bubble classes was negated by the numerical effort increase with increasing number of bubble size classes. The investigations were performed also for the test 107 (J_L=1.017 m/s, J_G=0.14 m/s) with the same results.

5.2. Application of the inhomogeneous MUSIG-Model

In addition to the studies described in chapter 5.1, the current chapter reconsiders the previous case with the inclusion of the mass exchanged by bubble coalescence and break-up, i.e. the change of the bubble size distribution was investigated. The bubble size distribution at the inlet was given and adapted to experimental results. The development of the size distribution and of the radial gas profile along the flow was subject of the model studies described in this section here.

5.2.1. Test MTLoop 118

Fig. 9 shows the measured size distribution at the inlet and the outlet of the tube. In the actual test case the mean Sauter diameter between inlet and outlet remains almost constant, whereas the size distribution is expanded by both coalescence and break-up.
Two dispersed phases were simulated. The first phase was

further assigned to 12 and the second phase to 22 sub-size MUSIG-groups. Over all 32 groups having a equidistant size step of 0.5 mm were simulated.

The bubble break-up model of Luo and Svendsen (1996) and the bubble coalescence model of Prince and Blanch (1990) were applied. The results indicated that tuning coefficients as dimensionless factors of the mass transfer rates F_B for bubble break-up and F_C for bubble coalescence had to be set to harmonize the mechanisms of break-up and coalescence. Best agreement to the measurements was found for a break-up coefficient F_B =0.25 and a coalescence coefficient F_C =0.05. All further calculations for air/water in a vertical tube were performed using these same set of coefficients.

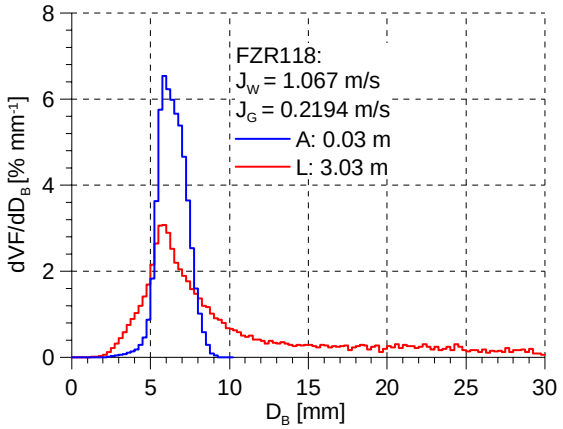

Figure 9: Measured development of the bubble size distribution from the inlet (level A) to the outlet (level L)

Fig. 10 presents the development over the tube height of the bubble size distribution and of the radial gas profiles. On the left side in each bubble size distribution also the distribution at the injection is presented (blue). During each measurement run also gas fraction profiles assigned to a certain bubble size region are determined. The radial gas profiles on the right side show also the measured radial gas profiles for d_b<6 mm (blue stars) and d_b>6 mm (green stars) and compares to the calculated profiles of the calculations (solid lines).

Further investigations but not presented here with 3 and 4 dispersed phases show that an increasing number of dispersed phases does not improve the agreement to the measurements. On the other side the computational effort is increased and it is becoming more difficult to achieve a certain convergence level.

5.2.2. Test TOPFLOW 118

In the TOPFLOW test, bubbles were injected from the side walls through 4 mm nozzles into a tube of diameter 195.3 mm. The bubble size distribution near the inlet shows large fractions of large bubbles (blue size distribution left side). During the upward flow through the tube the size distribution is shifted towards lower values. Thus the development of the bubble size distribution is mainly determined by break-up processes. Bubble coalescence plays only a minor role at the flow conditions of the experimental test. Fig. 11 shows the bubble size distribution and radial gas profiles for the test case TOPFLOW 118 for a quite low distance from the gas injection of 0.335 m and at a distance of 7.802 m. Note that only two dispersed phases were defined for the numerical model. 20 sub-size groups were then specified the first 2 sub-size groups assigned to the first dispersed phase and the other 18 to the second dispersed phase. The bubble size diameter was defined up to 60 mm, the size step between the sub-size groups amounts to 3 mm. Test calculations have shown setting the break-up coefficient to F_B=0.25 and the coalescence coefficient to F_C=0.05 yields the best agreement for this flow situation of air water flow in vertical pipes. Both the shift of the bubble size distribution (Fig. 11 left side) and the core peak gas volume fraction profile are well reproduced by the calculations.

6. Summary and conclusions

Applying the inhomogeneous MUSIG approach a more deep understanding of the flow structure is possible. For upward two phase flow in vertical pipes the core peak in the cross sectional gas fraction distribution could be reproduced very well. While the closure models on bubble forces, which are responsible for the simulation of bubble migration are in agreement with the experimental observations, clear deviations occur for bubble coalescence and break-up. The presently applied models describing bubble break-up and coalescence could be proved as weak points in numerous CFD analyses of vertical upward two phase pipe flow. Further work on this topic is under way.

Acknowledgements

The work is carried out as a part of current research projects funded by the German Federal Ministry of Economics and Labour, project numbers 150 1265 and 150 1271. The authors express their gratitude to the technical TOPFLOW team.

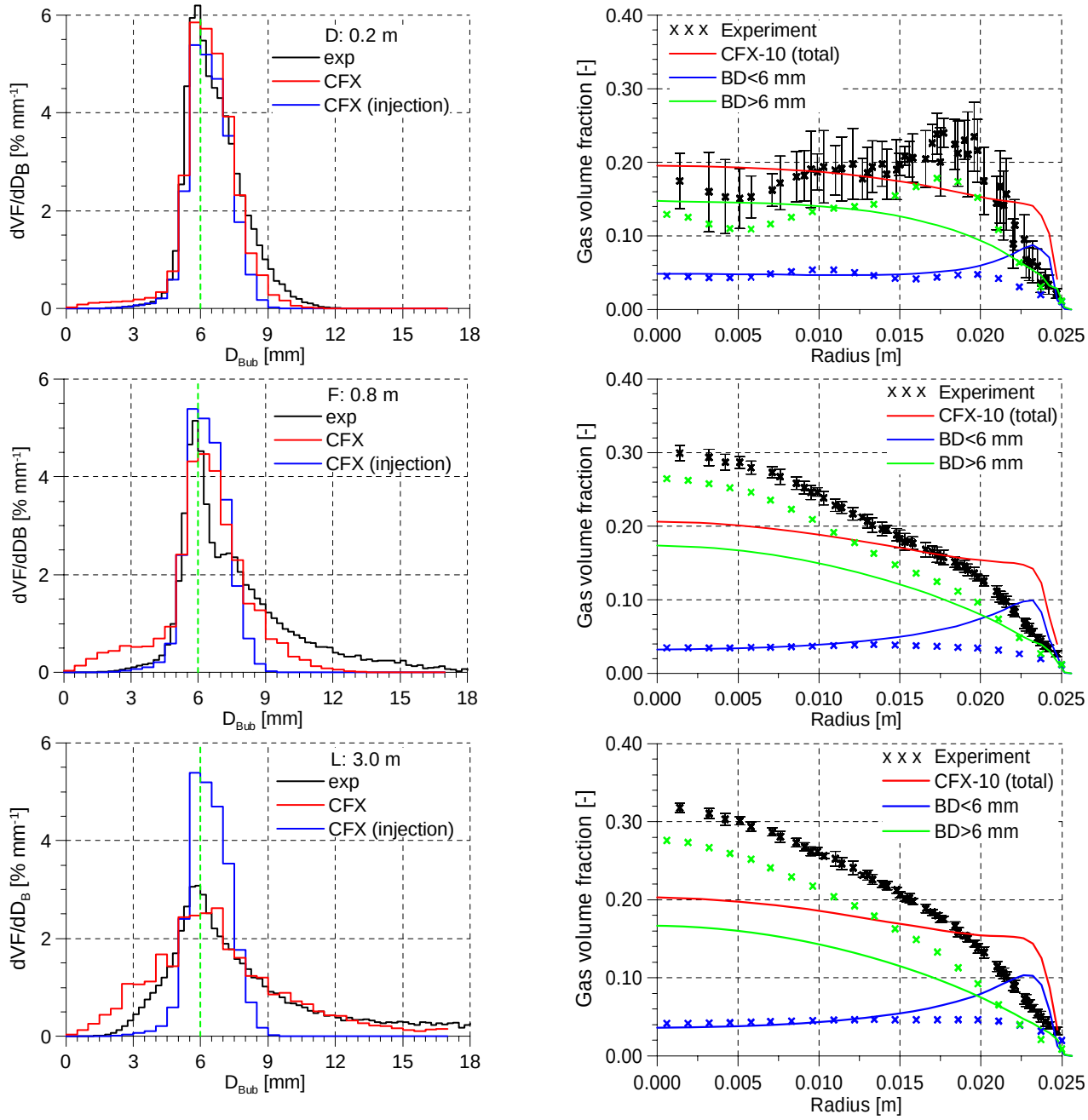

Figure 10: Development of the bubble size distribution (left) and the radial gas fraction profiles (right) of the simulation of the test case MT-Loop 118 (J_L=1.017 m/s; J_G=0.2194 m/s) 2 dispersed phases, 34 MUSIG Groups (F_B=0.25, F_C=0.05)

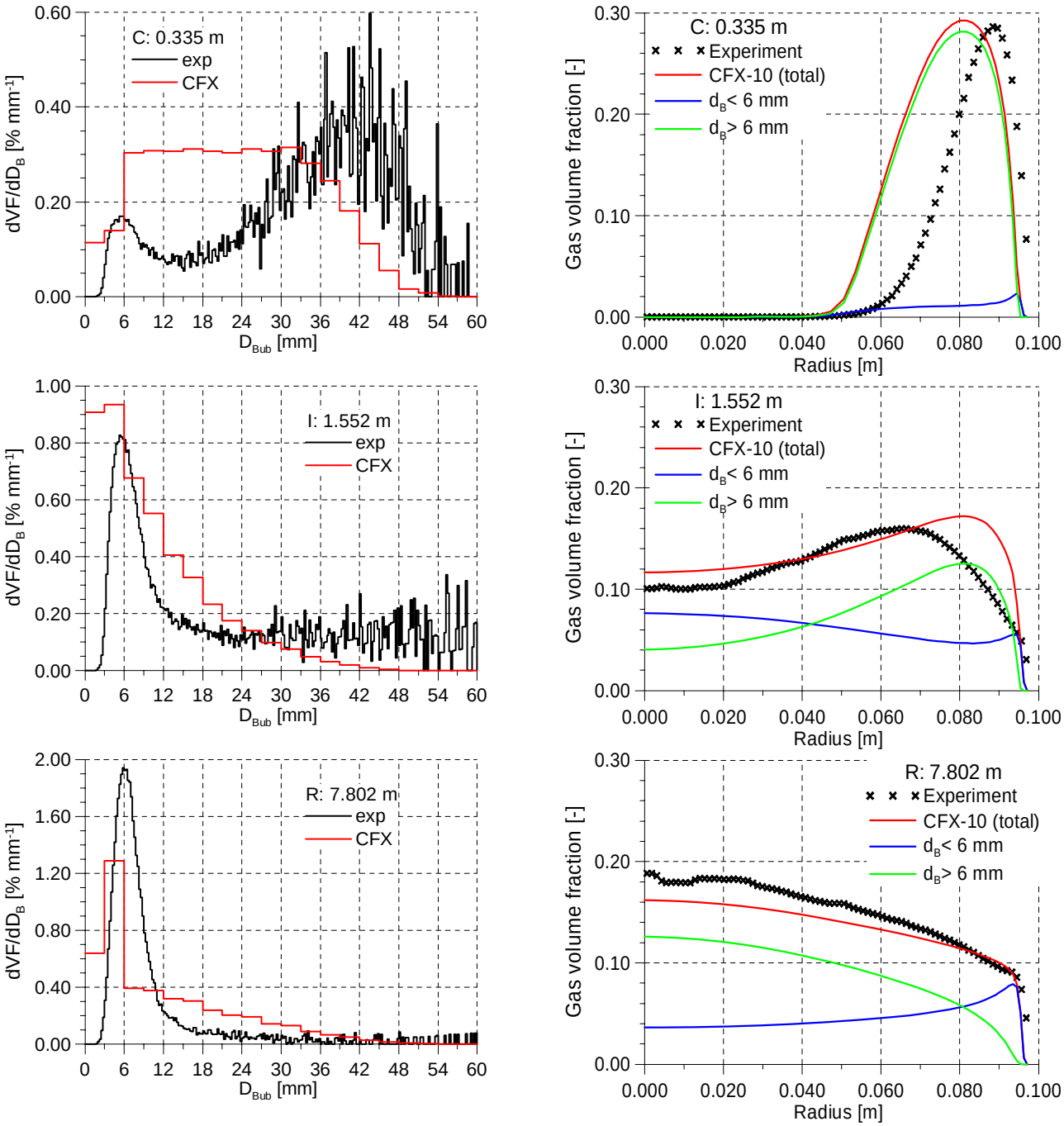

Figure 11: Bubble size distribution (left) and the radial gas fraction profiles (right) of the simulation of the test case TOPFLOW 118 at the distance levels from the gas injection C and R (J_L=1.017 m/s; J_G=0.2194 m/s) (Break-up coefficient F_B=0.25, Coalescence coefficient F_C=0.05)

References

Bothe, D., M. Schmidtke, H.-J. Warnecke (2006) VOF-Simulation of the Lift Force for Single Bubbles in a Simple Shear Flow, Chem. Eng. Technol. 29, No. 9, 1048–1053

Burns, A. D., T. Frank, I. Hamill J.-M. Shi, The Favre Averaged Drag Model for Turbulent Dispersion in Eulerian Multi-Phase Flows, 5th International Conference on Multiphase Flow, ICMF'04, Yokohama, Japan, May 30–June 4, 2004, Paper No. 392.

Ervin, E.A., Tryggvason, G. (1997). The rise of bubbles in a vertical shear flow, J.l of Fluids Engineering, vol. 119, pp. 443-449.

Frank, T., Zwart, P.J., Shi, J.-M., Krepper, E., Rohde, U. (2005). Inhomogeneous MUSIG Model – a Population Balance Approach for Polydispersed Bubbly Flows, International Conference "Nuclear Energy for New Europe 2005", Bled, Slovenia, September 5-8, 2005.

Frank, Th., Zwart, P.J., Krepper, E., Prasser, H.-M., Lucas, D., (2006). Validation of CFD models for mono- and polydisperse air-water two-phase flows in pipes, OECD/NEA International Workshop on The Benchmarking of CFD Codes for Application to Nuclear Reactor Safety (CFD4NRS), 05.-09.09.2006, Garching, Deutschland, OECD/NEA, 05.-09.09.2006, Garching, Germany.

Krepper, E.; Lucas, D.; Prasser, H.-M. (2005) On the modelling of bubbly flow in vertical pipes, Nuclear Engineering and Design 235 (2005) 597-611

Krepper, E., Beyer, M., Frank, Th., Lucas, D. (2007) Application of a Population Balance Approach for Polydispersed Bubbly Flows, 6th Int. Conf. on Multiphase Flow Leipzig 2007, paper 378

Lo S. (1996). Application of the MUSIG model to bubbly flows, AEAT-1096, AEA Technology, June 1996.

Luo, H. and Svendsen, H.F. (1996), Theoretical model for drop and bubble break-up in turbulent flows, AIChEJ, 42, 5, pp. 1225-1233

Prasser, H.-M., Krepper, E., Lucas, D., (2002). Evolution of the two-phase flow in a vertical tube - decomposition of gas fraction profiles according to bubble size classes using wire-mesh sensors. International Journal of Thermal Sciences, 41 (2002) 17-28.

Prasser, H.-M.; Beyer, M.; Carl, H.; Gregor, S.; Lucas, D.; Pietruske, H.; Schütz, P.; Weiss, F.-P. (2007) Evolution of the structure of a gas-liquid two-phase flow in a large vertical pipe, Nuclear Engineering and Design (accepted for publication)

Prince, M.J. and Blanch, H.W. (1990), Bubble coalescence and break-up in air-sparged bubble columns, AIChEJ, 36, No 10, pp. 1485-1499

Shi, J.-M., Zwart, P.-J., Frank, T., Rohde U. and Prasser, H.-M. (2004). Development of a multiple velocity multiple size group model for poly-dispersed multiphase flows. In Annual Report of Institute of Safety Research. Forschungszentrum Rossendorf, Germany, 2004.

Tomiyama, A. Sou, I. Zun, I. Kanami, N. Sakaguchi, T. (1995). Effects of Eötvös number and dimensionless liquid volumetric flux on lateral motion of a bubble in a laminar duct flow, Advances in Multiphase Flow, pp. 3-15.

Tomiyama A. (1989): "Struggle with computational bubble dynamics", ICMF'98, 3rd Int. Conf. Multiphase Flow, Lyon, France, pp. 1-18, June 8.-12. 1998.

Wellek, R.M., Agrawal, A.K., Skelland, A.H.P., (1966). Shapes of liquid drops moving in liquid media, AIChE Journal, vol. 12, pp. 854-860.

Zwart, P., A. Burns, A. and Montavon C.. (2003). Multiple size group models. Technical report, AEA Technology plc, Novermber, 2003. CFX-5.7.